Polymer Journal, Vol. 31, No. 6, pp 542—549 (1999)

^{13}C NMR Relaxation of Poly(*t*-butyl crotonate) in Solution. Effects of β-Substitution on Local Chain Motions

Shinichi YAMAZAKI,† Eisaku OKADA, Yoshio MUROGA, Ichiro NODA, and Akihiro TSUTSUMI*

Department of Applied Chemistry, Graduate School of Engineering, Nagoya University, Furo-cho, Chikusa-ku, Nagoya 464-8603, Japan
** Division of Applied Physics, Graduate School of Engineering, Hokkaido University, Kita-13, Nishi-8, Kita-ku, Sapporo 060-8628, Japan*

(Received December 15, 1998)

ABSTRACT: Measurement of ^{13}C spin-lattice relaxation times, T_1, and nuclear Overhauser effects, NOE, was made as a function of temperature at two magnetic fields for poly(*t*-butyl crotonate), PTBC, and poly(*t*-butyl methacrylate), PTBM, in toluene-d_8 to study the effects of β-substitution on local chain motions. For main chain carbons of PTBC and PTBM, experimental T_1 and NOE data were well reproduced by the Dejean–Lauprêtre–Monnerie (DLM) model in the entire temperature range. The model parameters thus obtained differed between PTBC and PTBM. For methyl carbons in the *t*-butyl ester group, the experimental data were analyzed by the models combining the DLM model and multiple internal rotations. The model parameters were almost the same for the two polymers. These results indicate that β-substitution affects the local motion of main chains as well as chain stiffness, but does not significantly affect the local motion of methyl carbons at the ends of side-chains. The correlation between the local dynamics of various polymer chains and chain stiffness is discussed.

KEY WORDS ^{13}C NMR Relaxation / Poly(*t*-butyl crotonate) / Spin-Lattice Relaxation Time / Nuclear Overhauser Effect / β-Substitution / Local Chain Motions / Chain Stiffness /

Static properties such as unperturbed conformation of polymer chains or chain stiffness have been extensively studied theoretically and experimentally,[1,2] whereas, dynamic properties such as local chain motions of polymer chains have been recently studied by various relaxation experiments such as NMR relaxation,[3-5] dielectric relaxation,[6,7] and time-resolved fluorescence.[8] Since both properties are considered closely related,[5,7] it is interesting to study the relationship between them. Previous papers showed by light scattering,[9] intrinsic viscosity[10] and small-angle X-ray scattering measurements[11] that the persistence length of poly(*t*-butyl crotonate), PTBC, is much longer than that of poly(*t*-butyl methacrylate), PTBM. That is, steric hindrance between β-methyl and *t*-butyl ester groups makes polymer chains stiff. Thus, the present work studied the effects of β-substitution on local chain motions, using both PTBC and PTBM.

The NMR relaxation method is quite useful because it provides detailed information about molecular motion of different parts of chain through the spectral density function which is the Fourier transformation of correlation function of the relaxing dipoles in different environments of chains. This work thus studied ^{13}C NMR relaxation such as spin-lattice relaxation time T_1 and nuclear Overhauser effect, NOE, of PTBC and PTBM at two magnetic field (67.8 and 125.7 MHz) as a function of temperature.

In polymer chains with side-chains, local dynamical processes occur in short segments of both main and side chains. There are various models that describe local chain motion in terms of conformational transition, multiple internal rotation, etc. For main chain motions, Dejean, Lauprêtre, and Monnerie modified the Hall–Weber–Helfand (HWH) model describing the main chain motions in terms of the conformational transitions[12,13] by introducing libration motion of the C–H vector.[14] The Dejean–Lauprêtre–Monnerie (DLM) model is in good agreement with experimental T_1 and NOE data for various polymers in solution or bulk.[14-21] The interesting features of this model include correlation times for damping (single conformational transition), propagation (correlated pair conformational transition) and libration, which can be related with chain stiffness. That is, the degree of damping and propagation along the main chain may be related with the chain stiffness and degree of libration motion may be related to steric environment around a C–H unit. For side-chain motion, the relaxation is more complicated owing to superposition of main chain motions and multiple internal rotations in the side-chain. Several models for multiple internal rotations such as free rotational diffusion, restrict rotational diffusion and three site jump models have been proposed.[22-29] In this work, we analyzed experimental ^{13}C NMR data of main and side chains by the DLM model and the multiple internal rotations, respectively, to study the effects of β-substitution or chain stiffness on the local chain motions.

EXPERIMENTAL

PTBC and PTBM samples used here were prepared by anionic polymerization in our laboratory. Details of the preparation are described in a previous paper.[30] Molecular weights were $M_w = 128000$ and 32000, respectively, determined by GPC calibrated with standard polystyrenes of Tosoh Co. Ltd. and tacticity is atactic. The polymer concentration was 10 wt/vol% in toluene-d_8, purchased from Aldrich Chemical Co. In the main chain carbons in the repeating unit of PTBC, a carbon attached with *t*-butyl ester group is identified as α-methine carbon and another carbon as β-methine carbon (see Figure 1).

^{13}C NMR relaxation experiments were performed with

† To whom correspondence should be addressed.

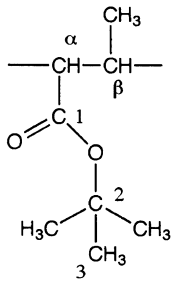

Figure 1. Labeling scheme of carbon atoms in the repeating unit of PTBC.

Varian unity INOVA 500 and JEOL FX-270 NMR instruments operating at 125.7 and 67.8 MHz for carbon resonance frequency, respectively. Temperatures were regulated within ± 1 K by a controller. T_1 was measured by conventional inversion recovery using 180°–τ–90° pulse sequence. 2000—4000 acquisitions were accumulated for a set of 12—14 arrayed τ and the delay times between pulse cycles were 5 times longer than maximum T_1. T_1 was determined by fitting the observed data to a nonlinear exponential function. NOE was evaluated as the ratio of ^{13}C signal intensities obtained by continuous ^{1}H decoupling to those obtained by inverse gate decoupling. The delay times for NOE experiments were 10 times longer than maximum T_1. All sample solutions were degassed, though the experimental data were not seriously affected for the system having a short relaxation time such as polymer solution.[31] The relative error of measured T_1 and NOE values was estimated to be lower than 10 and 15%, respectively.

THEORETICAL BACKGROUND

Assuming a purely ^{13}C–^{1}H dipolar–dipolar relaxation mechanism, we have the following equations for spin-lattice relaxation time, T_1, and NOE, under the condition of complete proton decoupling.[22]

$$\frac{1}{T_1}=\frac{N}{10}\left[\frac{\mu_0\hbar\gamma_H\gamma_C}{4\pi r^3}\right]^2[J(\omega_H-\omega_C)+3J(\omega_C)+6J(\omega_H+\omega_C)] \quad (1)$$

$$\mathrm{NOE}=1+\frac{\gamma_H}{\gamma_C}\left[\frac{6J(\omega_H+\omega_C)-J(\omega_H-\omega_C)}{J(\omega_H-\omega_C)+3J(\omega_C)+6J(\omega_H+\omega_C)}\right] \quad (2)$$

where N, μ_0, and r are the number of direct bonded proton, permeability in vacuum, C–H internuclear distance (0.109 nm),[32] respectively, $\hbar=h/2\pi$ with h being Planck constant, and γ_H, γ_C, ω_H, and ω_C are the magnetogyric ratios and Larmor frequencies of ^{1}H and ^{13}C, respectively. The spectral density function, $J(\omega)$, is obtained by the Fourier transformation of the correlation function, $G(t)$, derived on the basis of motional models.

$$J(\omega)=\frac{1}{2}\int_{-\infty}^{\infty}G(t)\exp(i\omega t)\mathrm{d}t \quad (3)$$

MOTION MODELS

Main Chain Motion

The DLM model[12] describes local chain motions in terms of conformational transition and libration, which well explain T_1 and NOE data for various polymers in solution and bulk.[12,15–21] The spectral density function, $J(\omega)$, of the DLM model is given by

$$J(\omega)=\frac{1-f}{(\alpha+i\beta)^{1/2}}+\frac{f\tau_2}{1+\omega^2\tau_2^2} \quad (4)$$

with

$$\alpha=\frac{1}{\tau_0^2}+\frac{2}{\tau_0\tau_1}-\omega^2 \quad (5)$$

and

$$\beta=-2\omega\left[\frac{1}{\tau_0}+\frac{1}{\tau_1}\right] \quad (6)$$

where τ_0, τ_1, τ_2, and f are correlation times for damping, propagation and libration, and relative weight of libration, respectively. According to the theory of Howarth,[33] f is given by,

$$1-f=\left[\frac{\cos\theta-\cos^3\theta}{2(1-\cos\theta)}\right]^2 \quad (7)$$

where θ is the libration angle of C–H vector.

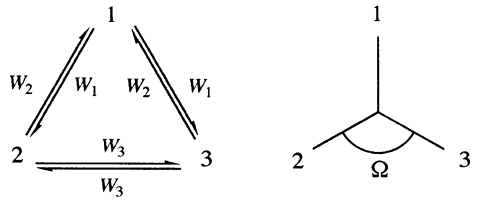

Figure 2. Schematic illustration of jump model.

Side-Chain Motion

The relaxation parameters, T_1 and NOE, in side-chain carbons are given by superposing both segmental motions in main chain and multiple internal rotational motions in the side-chain. Motion analysis for methyl carbon in the *t*-butyl ester group was performed by assuming the multiple internal rotations with two axes as described below. Internal rotations around the C_α–C_1O and C_1O–C_2 bonds in the *t*-butyl ester group cannot be evaluated without the following assumption, since there is no hydrogen attached to these bonds as shown in Figure 1, while the rotation around the C_1–O bond can be neglected because of conjugate nature of the bond. Therefore, we assumed internal rotational motion around C_α–C_1O and C_1O–C_2 bonds as the single rotation around the first axis, which is independent of temperature, *i.e.*, no activation energy, or constant, though, strictly speaking, this assumption may not be valid for relaxation for carbonyl and quaternary carbons in the ester groups because of steric hindrance with the carbonyl groups.

Free rotational diffusion and equivalent three site jump models are useful for describing local motion for end of side-chains[22,23] or internal rotational motion around C_2–C_3 bonds as the second axis, though the more elaborate analysis was performed for local motions of side-chain.[21] A schematic illustration of jump model is shown in Figure 2, where positions 1, 2, and 3 correspond to the three possible sites which are related to *trans*,

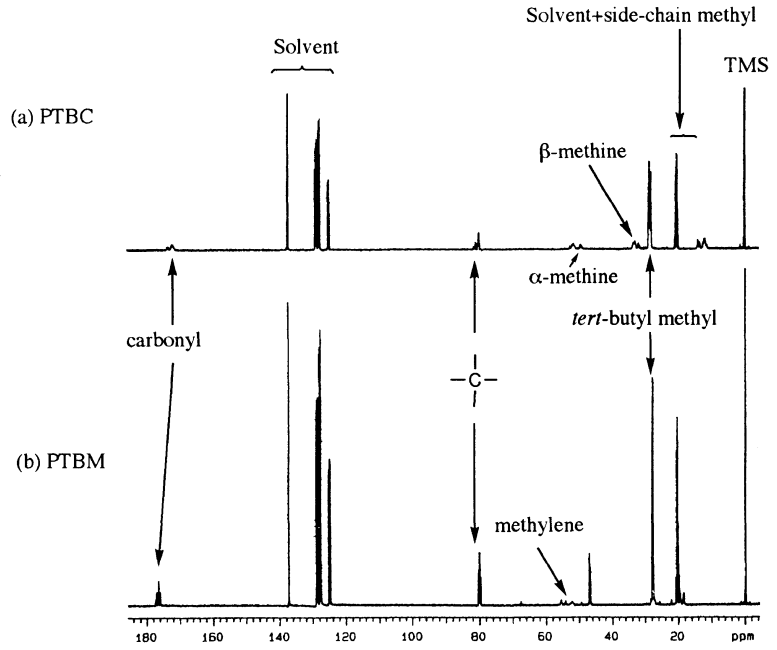

Figure 3. ^{13}C NMR spectra of PTBC (a) and PTBM (b) at 125.7 MHz.

gauche$^+$, and *gauche*$^-$ forms, and W_1, W_2, and W_3 are the respective jump rates (1→2 and 3), (2 and 3→1), and (2↔3) where $W_i = W_0 \exp(-E_i/RT)$ with E_i, R, and T the apparent activation energy between sites, gas constant and absolute temperatures, respectively. Ω is the angle between site 2 and 3 (120° for alkyl chain). The jump rates are related with internal correlation time τ_{ir} as $W_i = (6\tau_{ir})^{-1}$ for free rotational diffusion model and $W_i = (3\tau_{ir})^{-1}$ for an equivalent three site jump model, respectively.

FITTING PROCEDURE

Experimental T_1 and NOE data were analyzed by motional models as above. According to Helfand,[34] who applied the theory of Kramer[35] for the diffusion of a particle over a potential barrier to conformational transitions of polymer chains, the temperature dependence of the correlation time $\tau(T)$ is given by the Arrhenius type as,

$$\tau(T) = A \exp(E_a/RT) \tag{8}$$

with $A = \eta c$ where η, c, and E_a are solvent viscosity, molecular constant and apparent activation energy, respectively. In the fitting procedure, A and E_a were treated as adjustable parameters.

T_1 and NOE are fitted simultaneously at both magnetic fields as a function of temperature. At first the parameters, A, E_a, f, τ_0/τ_1, and τ_1/τ_2 in the DLM model were fitted manually for main chain carbons, and then the parameters of the internal rotation models, W_0 and E_i, were fitted for the side-chain carbons while the fitting parameters obtained for the main chain carbons were fixed.

RESULTS

Figure 3 shows the ^{13}C NMR spectra of PTBC (a) and PTBM (b) in toluene-d_8 at 125.7 MHz. Chemical shift was measured from tetramethylsilane (TMS) resonance as an internal reference and the peaks were assigned as reported previously.[36] Since the peak of β-methyl carbon in the side-chain of PTBC is overlapped by the solvent peaks at about 10—20 ppm, T_1 and NOE of this carbon could not be accurately determined. In this work, therefore, we examined only segmental motion of main chain carbons and multiple internal rotational motion of methyl carbons in *t*-butyl ester groups.

Tables I and II summarize ^{13}C T_1 and NOE data as a function of temperature at the two magnetic fields for PTBC and PTBM, respectively. The data were obtained for the major component of stereo-sequence. The values obtained for minor components almost agree with those of major one within experimental errors. The data in these tables indicate the following specific features. For the main chain carbons of both PTBC and PTBM, T_1 lies on the higher correlation time side of the T_1 minimum, and this is remarkable at the higher magnetic field. T_1 increases with decreasing temperature at both magnetic fields. NOE is significantly smaller than the maximum value (3.0) obtained at the extreme narrowing limit and seem to have a minimum at the lower magnetic field. This implies that the segmental motion in the main chain cannot be explained by the correlation function having a single correlation time.[21]

For side-chain carbons, T_1 of PTBC and PTBM are larger than those of main chain carbons at the entire temperature range. This implies that there is a contribution of multiple internal rotations to the side-chain motions in addition to the segmental motion in the main chain. T_1 of both PTBC and PTBM increase with temperature, but the former is larger. NOE of PTBC is slightly smaller than for PTBM.

DISCUSSION

Figures 4, 5, and 6 show the best fitting curves of T_1 and NOE *vs.* temperature, calculated by the parameters

Table I. Experimental T_1 (ms) and NOE[a] data of PTBC as a function of temperature in two magnetic fields

Temp/K	Main chain carbon				Side-chain carbon	
	α-CH		β-CH		*t*-Butyl CH_3	
	125.7 MHz	67.8 MHz	125.7 MHz	67.8 MHz	125.7 MHz	67.8 MHz
307	461 (1.52)	230 (1.98)	449 (1.67)	231 (1.94)	482 (2.40)	359 (2.40)
313	462 (1.79)	246 (1.80)	438 (1.72)	238 (1.86)	498 (2.40)	373 (2.44)
323	455 (1.92)	208 (1.61)	437 (1.98)	214 (1.65)	569 (2.44)	383 (2.47)
333	451 (1.89)	211 (1.46)	452 (1.75)	229 (1.62)	604 (2.48)	512 (2.44)
343	415 (1.64)	253 (1.49)	416 (1.64)	222 (1.45)	693 (2.48)	601 (2.40)

[a] Values in parentheses.

Table II. Experimental T_1 (ms) and NOE[a] data of PTBM as a function of temperature in two magnetic fields

Temp/K	Main chain carbon		Side-chain carbon	
	CH_2		*t*-Butyl CH_3	
	125.7 MHz	67.8 MHz	125.7 MHz	67.8 MHz
303	207 (1.68)	98 (1.75)	383 (2.35)	267 (2.52)
313	196 (1.69)	122 (1.70)	431 (2.45)	282 (2.56)
323	184 (1.75)	94 (1.54)	482 (2.55)	315 (2.56)
333	163 (1.60)	88 (1.58)	542 (2.59)	482 (2.58)
343	158 (1.55)	71 (1.65)	614 (2.49)	558 (2.53)

[a] Values in parentheses.

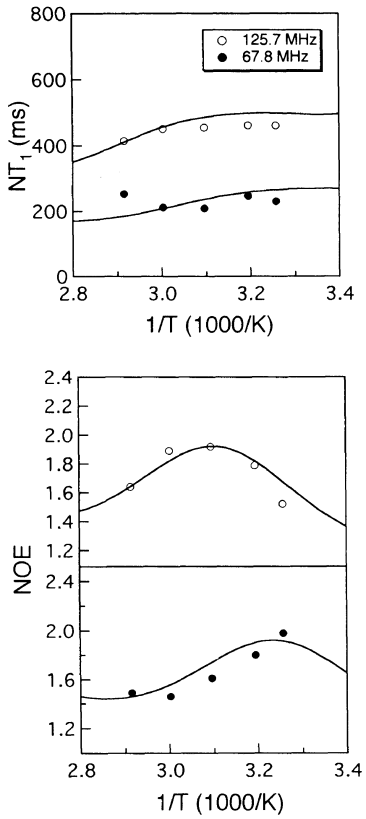

Figure 4. Temperature dependence of T_1 and NOE for α-methine carbon of PTBC. Solid lines calculated by the DLM model with the parameters listed in Table III.

of the DLM model listed in Table III for α-, β-methine carbons of PTBC, and methylene carbon of PTBM, respectively. In the entire temperature range, experimental T_1 and NOE are in good agreement with the DLM model for both polymers. As shown in Table III, there is no significant difference between the model parameters obtained for α- and β-methine carbons of PTBC. This implies that the segmental motions of α- and β-methine carbons are governed by the same mechanism of local dynamics. This is reasonable because there is no significant difference in neighboring environments for α- and β-methine carbons.

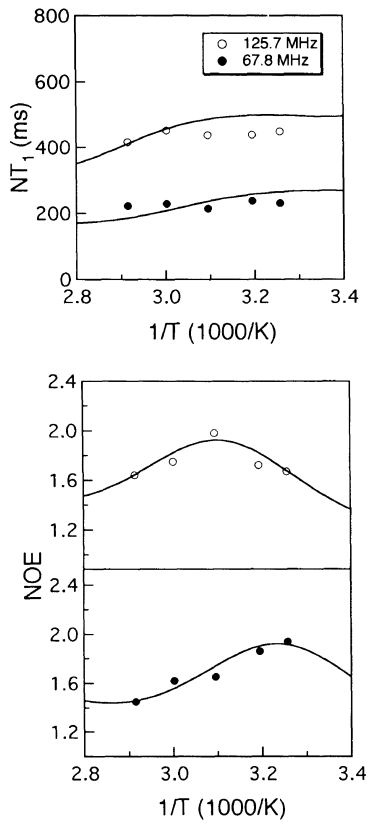

Figure 5. Temperature dependence of T_1 and NOE for β-methine carbon of PTBC. Solid lines calculated by the DLM model with the parameters listed in Table III.

Let us compare the parameters of PTBC and PTBM in Table III. The correlation time ratio τ_0/τ_1 of the former (1.7) is smaller than that of the latter (2.0). Since the difference in molecular architecture between the two polymers is in the position of methyl unit on the main chains and the former chain is stiffer than the latter chain due to the steric hindrance between β-methyl and *t*-butyl ester groups, this implies that PTBC having the stiffer chain has smaller correlation time ratio.

Thus, let us examine the relationship between the correlation time ratio and the chain stiffness for other polymers having similar molecular architectures, *i.e.*, polyacrylate or polymethacrylate derivatives and vinyl polymers. The chain stiffness can be represented by the characteristic ratio, $C_\infty = \langle r^2 \rangle_0 / nl^2$, where $\langle r^2 \rangle_0$, n and l are the unperturbed mean square end-to-end distance, degree of polymerization and monomer length, respectively. Table IV lists the correlation time ratios and characteristic ratios of the polymers. Here, the characteristic ratio of PTBC was evaluated from the persistence length (*ca.* 1.9—3.1 nm) measured by small angle X-ray scattering.[11] Although the characteristic ratios are unknown for poly(isobutyl methacrylate) (PIBM), poly(naphthyl acrylate) (PNA), and poly(1-naphthylmethyl acrylate) (PNMA), the values of PIBM and PNA may be close to that of PTBM because they have bulky groups similar to *t*-butyl ester, while PNMA may be smaller because a methyl unit intervenes between a carboxyl group and a naphthalene unit. Figure 7 shows a comparison between the correlation time and characteristic ratios. Roughly speaking, this implies that the stiffer the chain is, the smaller the correlation time ratio is. This is understandable because the smaller correlation time ratio means that the propagation of local motion associated with τ_1 is more restricted by damping associated with τ_0.

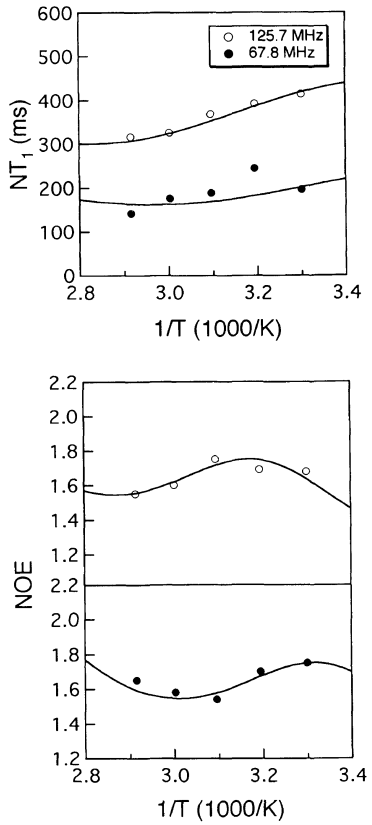

Figure 6. Temperature dependence of T_1 and NOE for methylene carbon of PTBM. Solid lines calculated by the DLM model with the parameters listed in Table III.

We compared the activation energy E^* associated with a potential barrier for conformational transition with the chain stiffness. If eq 8 is valid for the conformational transitions, E^* is given by

$$E^* = E_a - E_\eta \tag{9}$$

where E_η is the activation energy of solvent viscosity, expressed as $\eta = B\exp(E_\eta/RT)$ with B a constant. As reported by Gisser *et al.*,[40] eq 8 is not valid for ordinary flexible chains, and the correlation times are proportional to η^α ($\alpha = 0.41$). In this case we have

$$E^* = E_a - \alpha E_\eta \tag{10}$$

In Table IV E_a and E^* are listed, and a comparison

Table III. Fitting parameters of the DLM model for main chain carbons of PTBC and PTBM

	τ_0/τ_1	τ_1/τ_2	E_a/kJ mol^{-1}	$10^{15}A$/s	θ
PTBC-α	1.7	60	38.9	7.4	30.5
PTBC-β	1.7	60	38.9	7.4	30.5
PTBM	2.0	30	36.4	7.4	30.5

Table IV. Correlation time ratio, activation energy, and characteristic ratio for various polymers

	τ_0/τ_1	E_a/kJ mol^{-1}	E^{*a}/kJ mol^{-1}	C_∞[b]	ref
PTBC	1.7	38.9	29.9—35.2	19.7±4.5	This work
PTBM	2	36.4	27.4—32.7	10.9	This work
Poly(isobutyl methacrylate) PIBM	2	36.4	27.4—32.7	Unknown	21
Poly(vinyl methyl ether) PVME	2	15.1	7.7—12.1	10.0	12
Poly(naphthyl acrylate) PNA	3	24.0	12.0—19.1	Unknown	37
Poly(butyl methacrylate) PBMA	5	25.0	16.0—21.3	8.2±0.4	38
Poly(hexyl methacrylate) PHMA	5	33.0	24.0—20.3	11.1±1.0	38
Poly(1-naphthymethyl acrylate) PNMA	7	25.0	11.3[c]	Unknown	39
Poly(vinyl chloride) PVC	7	23.9	13.7—19.7	7.7±1.0	18
Poly(2-vinyl pyridine) P2VP	8	18.5	11.1—15.5	8.6±1.4	19
Poly(vinyl alcohol) PVA	10	30.9	13.4—23.7	8.3	20

[a] Largest and smallest values evaluated by eq 9 and 10, respectively. [b] Reference 2 except for PTBC. [c] Equation 9 is valid for this polymer.

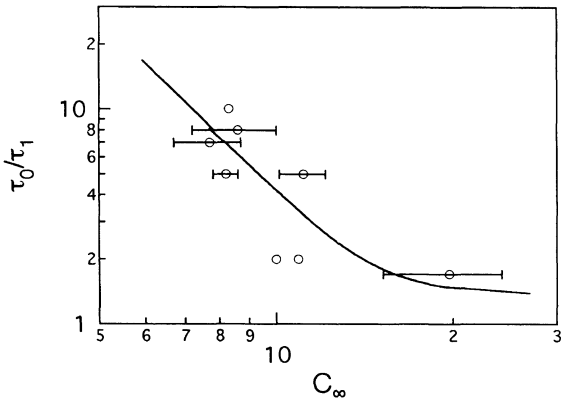

Figure 7. Plots of the correlation time ratio τ_0/τ_1 *vs.* characteristic ratio C_∞. A solid line is drawn as eye guide.

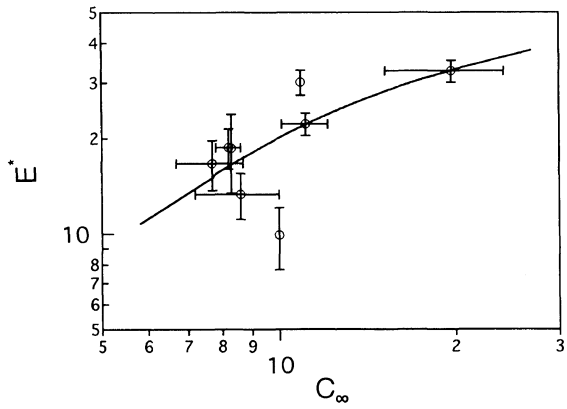

Figure 8. Plots of activation energy E^* for conformational transition *vs.* characteristic ratio C_∞. A solid line is drawn as eye guide.

between E^* and C_∞ is shown in Figure 8. It is of much interest that there is a correlation between local chain motion and chain stiffness as shown in Figures 7 and 8 though the origins are different. The former is associated with activation energy of rotation of bonds, while the latter, with difference in the potential minimum.

The libration angle θ in Table III is the same for α-, β-methine carbons of PTBC and methylene carbon of PTBM, *i.e.*, 30.5°. This implies that libration motion is not affected by the segmental motions as the former is much faster than the latter.[21] As shown in Table III, another correlation time ratio τ_1/τ_2 of PTBC (60) is larger than that of PTBM (30). The propagation may thus be more suppressed for PTBC than for PTBM if we assume that the libration motion is the same for both polymers as above.

Following the method of Guillermo *et al.*,[41] $\log(NT_1/\omega_c)$ is plotted against $\log(\omega_c\tau_1)$ for PTBC and PTBM at the two Larmor frequencies in Figure 9. T_1 data superpose fairly well for both polymers. The superposition implies that the mechanism of local motions as reflected in the correlation function, $G(t)$, is independent of temperature, and justifies the above analysis.

Figures 10 and 11 show the temperature dependence of T_1 and NOE data for side-chain methyl carbons in *t*-butyl ester group of PTBC and PTBM, respectively. The solid and broken lines are theoretical values calculated by free rotational diffusion and equivalent

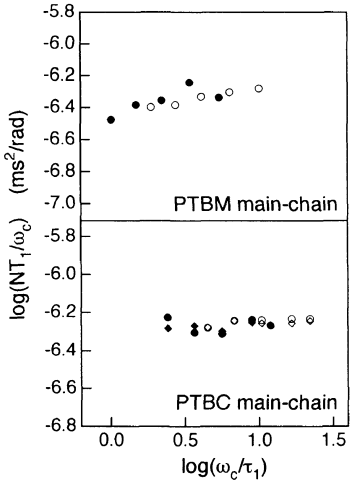

Figure 9. Frequency-temperature superposition of ^{13}C NT_1 for the main chain carbons of PTBC and PTBM. Open and filled symbols denote data of 125.7 and 67.8 MHz, respectively. Circle and diamond symbols are data of α-methine and β-methine carbons, respectively. τ_1 was evaluated using the DLM model.

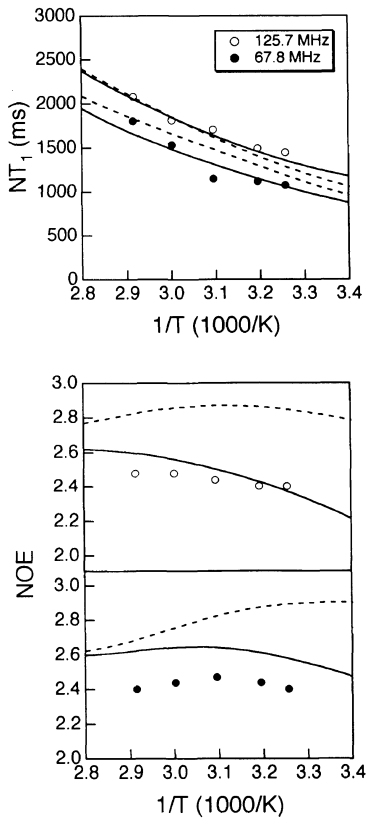

Figure 10. Temperature dependence of T_1 and NOE for methyl carbon in *t*-butyl ester group of PTBC. Solid and broken lines denote theoretical values of the free rotational diffusion model and three site jump model, respectively.

three site jump models, respectively. Here, we assume that the jump rate for the first axis, *i.e.*, around C_α–C_1O and C_1O–C_2 bonds is $W_0 = 3.30 \times 10^{11}\,s^{-1}$ for both PTBC and PTBM, determined so that the experimental data can be reproduced by the model. Even if this value is modified within $\pm 2.0 \times 10^{11}\,s^{-1}$, the fitting results would hardly be affected. The model parameters thus obtained are listed in Table V. As shown in Figures 10 and 11, T_1 data of both polymers are more satisfactorily

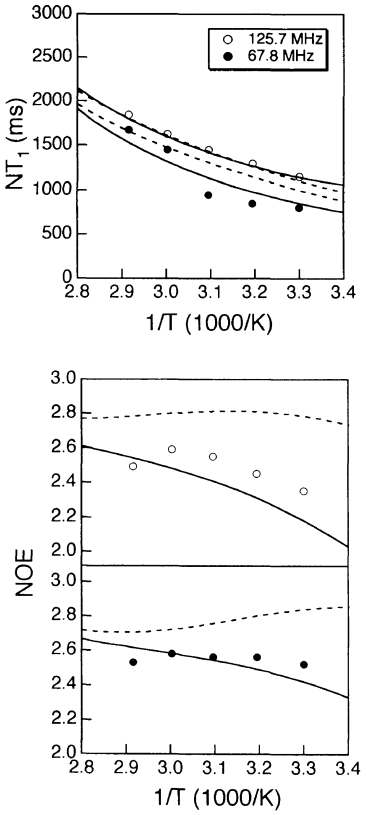

Figure 11. Temperature dependence of T_1 and NOE for methyl carbon in *t*-butyl ester group of PTBM. Solid and broken lines denote theoretical values of the free rotational diffusion model and three site jump model, respectively.

Table V. Fitting parameters of free rotational diffusion and three site jump models for side-chain carbons of PTBC and PTBM

	PTBC		PTBM	
	E_i	W_0	E_i	W_0
	kJ mol^{-1}	s^{-1}	kJ mol^{-1}	s^{-1}
Free rotational diffusion	19.0	2.60×10^{12}	20.8	3.80×10^{12}
Three site jump	15.4	1.57×10^{12}	14.0	7.20×10^{11}

reproduced by the free rotational diffusion model than the equivalent three site jump model, while the NOE data for PTBC at low fields and for PTBM at high fields somewhat deviate from the theoretical values of the free rotational diffusion model having the same parameters as those for fitting T_1 data, but the deviations are within experimental error and the temperature dependence is very similar to the experimental one. As shown in Table V, E_i and W_0 in the free rotational diffusion model are not much different between two polymers. This implies that the carbons themselves at the ends of side-chains rather freely move irrespective of chain stiffness if we assume that the side-chain rotates freely without the activation energy around the first axis. The overall side-chain motion is affected by the stiffness of main chain through the main chain motion.

CONCLUDING REMARKS

^{13}C NMR relaxation measurement of PTBC and PTBM in toluene-d_8 was carried out as a function of temperature at two magnetic fields. For main chain carbons of PTBC and PTBM, the T_1 and NOE data were well reproduced by the DLM model, and it was concluded that local motion of main chains is closely related to chain stiffness. For side-chain carbons, the free rotational diffusion model was suitable to describe the experimental data for PTBC and PTBM and this suggests that the ends of side-chains themselves rather freely move irrespective of chain stiffness.

REFERENCES

1. P. J. Flory, "Statistical Mechanics of Chain Molecules," Wiley, New York, N.Y., 1967.
2. J. Brandrup and E. H. Immergut, Ed., "Polymer Handbook," 3rd ed, John Wiley & Son, New York, N.Y., 1989.
3. F. Heatley, *Prog. NMR Spectrosc.*, **13**, 47 (1979).
4. F. Heatley, *Ann. Rep. NMR Spectrosc.*, **17**, 179 (1986).
5. F. A. Bovey and P. A. Mirau, "NMR of Polymers," Academic Press, San Diego, 1996.
6. W. H. Stockmayer, *Pure and Appl. Chem.*, **15**, 539 (1967).
7. J. P. Runt and J. J. Fitzgerald, Ed., "Dielectric Spectroscopy of Polymeric Materials: Fundamentals and Applications," American Chemical Society, Washington, D.C., 1997.
8. M. A. Winnik, Ed., "Photophysical and Photochemical Tools in Polymer Science: Conformation, Dynamics, Morphology," D. Reidel Pub., Dordrecht, 1985.
9. I. Noda, T. Imai, T. Kitano, and M. Nagasawa, *Macromolecules*, **14**, 1303 (1981).
10. I. Noda, Y. Yamamoto, T. Kitano, and M. Nagasawa, *Macromolecules*, **14**, 1306 (1981).
11. Y. Muroga, I. Sakuragi, and I. Noda, and M. Nagasawa, *Macromolecules*, **17**, 1844 (1984).
12. C. K. Hall and E. Helfand, *J. Chem. Phys.*, **77**, 3275 (1982).
13. T. A. Weber and E. Helfand, *J. Phys. Chem.*, **87**, 2881 (1983).
14. R. Dejean de la batie, F. Lauprêtre, and L. Monnerie, *Macromolecules*, **21**, 2045 (1988).
15. R. Dejean de la batie, F. Lauprêtre, and L. Monnerie, *Macromolecules*, **22**, 122 (1989).
16. A. Gérard, F. Lauprêtre, and L. Monnerie, *Polymer*, **36**, 3661 (1995).
17. D. J. Gisser, S. Glowinkowski, and M. D. Ediger, *Macromolecules*, **24**, 4270 (1991).
18. T. Radiotis, G. R. Brown, and P. Dais, *Macromolecules*, **26**, 1445 (1993).
19. S. Ravindranathan and D. N. Sathyanarayana, *Macromolecules*, **28**, 2396 (1995).
20. J.-M. Petit and X. X. Zhu, *Macromolecules*, **29**, 2075 (1996).
21. S. Ravindranathan and D. N. Sathyanarayana, *Macromolecules*, **29**, 3525 (1996).
22. D. E. Woessner, *J. Chem. Phys.*, **36**, 647 (1962).
23. D. Doddrell, V. Glusko, and A. Allerhand, *J. Chem. Phys.*, **56**, 3683 (1972).
24. W. Gronski and N. Murayama, *Macromol. Chem.*, **180**, 1119 (1979).
25. B. Perly, C. Chachaty, and A. Tsutsumi, *J. Amer. Chem. Soc.*, **102**, 1521 (1980).
26. A. Tsutsumi, *Mol. Phys.*, **37**, 11 (1979).
27. A. Tsutsumi and C. Chachaty, *Macromolecules*, **12**, 479 (1979).
28. R. J. Wittebort and A. Szabo, *J. Chem. Phys.*, **69**, 1922 (1978).
29. D. Ghesquiere, A. Tsutsumi, and C. Chachaty, *Macromolecules*, **12**, 775 (1979).
30. T. Kitano, T. Fujimoto, and M. Nagasawa, *Macromolecules*, **7**, 719 (1974).
31. G. C. Levy and I. R. Peat, *J. Magn. Reson.*, **18**, 500 (1975).
32. J. A. Pople and M. S. Gordan, *J. Amer. Chem. Soc.*, **89**, 4253 (1967).
33. O. W. Howarth, *J. Chem. Soc., Faraday Trans. 2*, **75**, 863 (1979).

34. E. Helfand, *J. Chem. Phys.*, **54**, 4651 (1971).
35. H. A. Kramers, *Physica*, **7**, 284 (1940).
36. Y. Muroga, I. Noda, and M. Nagasawa, *Macromolecules*, **13**, 1081 (1980).
37. A. Spyros, P. Dais, and F. Heartley, *Macromolecules*, **27**, 5845 (1994).
38. A. Spyros, P. Dais, and F. Heartley, *J. Polym. Sci., Polym. Phys. Ed.*, **33**, 353 (1995).
39. A. Spyros, P. Dais, and F. Heatley, *Macromolecules*, **27**, 6207 (1994).
40. D. J. Gisser, S. Glowinkowski, and M. D. Ediger, *Macromolecules*, **24**, 4270 (1991).
41. A. Guillermo, R. Dupeyre, and J. P. Cohen-Addad, *Macromolecules*, **23**, 1291 (1990).